Vibrational Characteristics and Aseismic Design of Sub-merged Bridge Piers

AUTHOR(S):

GOTO, Hisao; TOKI, Kenzo

Vibrational Characteristics and Aseismic Design of Sub-merged Bridge Piers

By

Hisao GOTO* and Kenzo TOKI*

(Received September 30, 1964)

This paper presents the dynamic water pressure on the cylindrical sub-merged bridge piers during earthquakes, and the vibrational characteristics of flexible sub-merged bridge piers. Moreover the authors discuss the damping effect of water and the aseismic design of sub-merged bridge piers consulting the theoretical and experimental analysis.

1. Introduction

Studies on dynamic water pressure during earthquakes have been carried out by H. M. Westergaard[1] and his results are well known as a formula for the dynamic water pressure acting on the unit length of under water structures. While T. Hatano[2] and S. Kotsubo[3] have investigated the dynamic water pressures on gravity dams and arch dams, R. M. Clough[4] has studied the rational estimation of the "virtual mass" using rigid prismatic bodies of various cross-sectional shape.

Although these investigations may give some suggestions for sub-merged bridge piers, there remain still some questions whether the results for wall structures are always applicable to columnar structures which are isolated in water and surrounded by water. Stillmore, it is said that the virtual mass is not always equal to the excluded mass of water by bodies and that some corrections are necessary for dumpy bodies. On the other hand, since the deflection of piers exerts influence upon the dynamic water pressure itself, the additional pressure should be considered with respect to the vibrational characteristics simultaneously.

The theoretical investigation is carried out on the dynamic water pressure on rigid cylindrical sub-merged bridge piers moving with arbitrary acceleration and vibrational characteristics, taking into consideration the additional dynamic

* Department of Transportation Engineering

water pressure caused by deflection and rocking of piers. Then the results of the theoretical analysis are compared with the ones of the model experiment.

2. Dynamic Water Pressure on Bridge Piers

2.1. Steady-state dynamic weter pressures

The dynamic water pressure is given by integrating Eq. (1) on velocity potential in cylindrical co-ordinates.

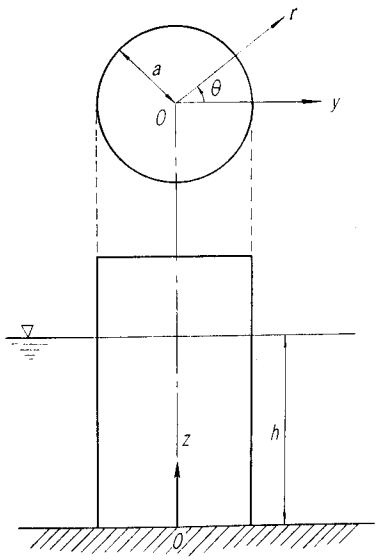

Fig. 1. Co-ordinates.

$$\frac{\partial^2\phi}{\partial r^2}+\frac{1}{r}\frac{\partial\phi}{\partial r}+\frac{1}{r^2}\frac{\partial^2\phi}{\partial\theta^2}+\frac{\partial^2\phi}{\partial z^2}-\frac{1}{c^2}\frac{\partial^2\phi}{\partial t^2}=0 \quad (1)$$

Boundary conditions in the system shown in Fig. 1 are as follows:

$$\left(\frac{\partial\phi}{\partial r}\right)_{r=a}=-\frac{\partial y}{\partial t}\cos\theta \quad (2)$$

$$\left(\frac{\partial\phi}{r\partial\theta}\right)_{\theta=0}=\left(\frac{\partial\phi}{r\partial\theta}\right)_{\theta=\pi}=0 \quad (3)$$

$$\left(\frac{\partial\phi}{\partial z}\right)_{z=0}=0, \quad \left(g\frac{\partial\phi}{\partial z}+\frac{\partial^2\phi}{\partial t^2}\right)_{z=h}=0 \quad (4)$$

Thinking of rigid piers under the simple harmonic motion, the steady-state solution of Eq. (1) satisfying boundary conditions has been derived. In the next place, writing the x-component and y-component of the dynamic water pressure per unit length of the pier as P_x and P_y respectively, leads to $P_x=0$ and P_y is expressed as follows:

$$\begin{aligned}P_y=&\sum_{m=1}^{s}\frac{8k_0g\rho\pi a}{\lambda_m}\frac{\sin\alpha_mh}{\sin 2\alpha_mh+2\alpha_mh}\frac{\sqrt{a_m^2+b_m^2}}{A_m^2+B_m^2}\cos\alpha_mz\cdot i\,e^{i(\omega t+\varepsilon_m)}\\&-\sum_{m=s+1}^{\infty}\frac{8k_0g\rho\pi a}{\lambda'_m}\frac{\sin\alpha_mh}{\sin 2\alpha_mh+2\alpha_mh}\frac{K_1(\lambda'_ma)}{K_0(\lambda'_ma)+K_2(\lambda'_ma)}\cos\alpha_mz\cdot i\,e^{i\omega t}\\&+\frac{8k_0g\rho\pi a}{\lambda_0}\frac{\sinh\alpha_0h}{\sinh 2\alpha_0h+2\alpha_0h}\frac{\sqrt{a_0^2+b_0^2}}{A_0^2+B_0^2}\cosh\alpha_0z\cdot i\,e^{i(\omega t+\varepsilon_0)}\end{aligned} \quad (5)$$

where

$$\lambda_m=\sqrt{\omega^2/c^2-\alpha_m^2}, \quad \lambda'_m=i\lambda_m, \quad \lambda_0=\sqrt{\omega^2/c^2+\alpha_0^2}$$

$$\tan\alpha_mh=-\omega^2/\alpha_mg, \quad \tanh\alpha_mh=\omega^2/\alpha_0g$$

$$A_m=J_0(\lambda_ma)-J_2(\lambda_ma), \quad B_m=Y_0(\lambda_ma)-Y_2(\lambda_ma), \quad \tan\varepsilon_m=b_m/a_m$$

$$a_m=A_mJ_1(\lambda_ma)+B_mY_1(\lambda_ma), \quad b_m=B_mJ_1(\lambda_ma)-A_mY_1(\lambda_ma)$$

and representations with suffix 0 are given by substitution λ_0 in λ_m.

Eq. (5) is similar to the expressions for the dynamic water pressure on wall structures. Notwithstanding, those expressions make the dynamic water pressure approach infinity under the condition which corresponds to the case λ_m or λ'_m equal to 0, in Eq. (5) it tends to the finite values for $\lambda_m=\lambda'_m=0$. Accordingly, it may be said that the resonance of the dynamic water pressure will never happen in the case of cylindrical piers isolated in water.

Neglecting the effect of surface wave and compressibility of water, Eq. (5) is reduced to

$$P_y = k_0\gamma_w\pi a^2\sum_{m=1}^{\infty}\frac{(-1)^{m-1}}{a_m h}\frac{4}{a_m a}\frac{K_1(a_m a)}{K_0(a_m a)+K_2(a_m a)}\cos a_m z \qquad (6)$$

Results of numerical computation are shown in Fig. 2 and compared with Westergaard's formula. This figure indicates that Eq. (6) is close to Westergaard's formula in the case of dumpy piers and that distribution and magnitude of dynamic water pressures are different from Westergaard's formula for slender piers. In the case of infinite water depth furthermore, P_y in Eq. (6) approaches to a constant $k_0\gamma_w\pi a^2$ which is derived in two dimensional analysis.

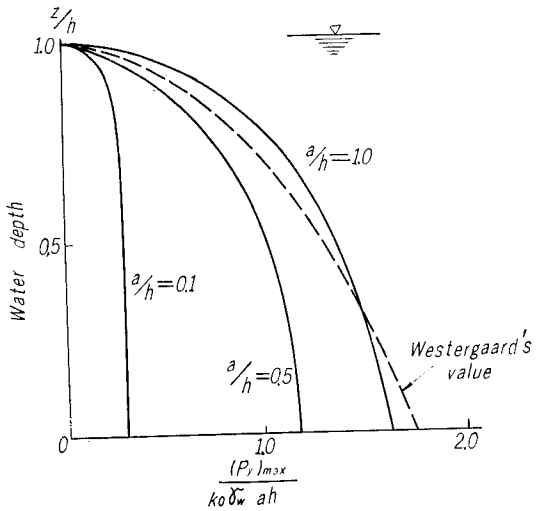

Fig. 2. Vertical distribution of the dynamic water pressure.

2.2. Transient dynamic water pressures

The theoretical aspects of the question were discussed in the preceding section on steady state dynamic water pressures. In this section, let us study a little further transient effects, particularly when the driving force itself varies so transient as actual earthquakes. To carry this out we shall set up the system in which the rigid cylindrical pier of radius a is fixed at the bottom in the large cylindrical pool of radius b and water depth h.

Let the pier start the motion at the time $t=0$ with acceleration $f(t)$, the dynamic water pressure p_a on cylinder surface can be derived as follows;

$$p_a = 4ac\rho \sum_{m=1}^{\infty} \sum_{l=1}^{\infty} \frac{(-1)^{m-1}\sqrt{\lambda_l^2+\alpha_m^2}\left\{\left(\frac{1}{\lambda_l a}\right)^2-\left(\frac{1}{\lambda_l b}\right)^2 \frac{J_1'(\lambda_l a)}{J_1'(\lambda_l b)}\right\}}{\alpha_m h\left[\left\{1-\left(\frac{1}{\lambda_l b}\right)^2\right\}\left\{\frac{J_1'(\lambda_l a)}{J_1'(\lambda_l b)}\right\}^2-\left\{1-\left(\frac{1}{\lambda_l a}\right)^2\right\}\right]} \cos\theta$$
$$\times \cos \alpha_m z \int_0^t f(\tau) \sin c\sqrt{\lambda_l^2+\alpha_m^2}(t-\tau)\, d\tau \qquad (7)$$

where λ_l is the root of $J_1'(\lambda a)Y_1'(\lambda b)-Y_1'(\lambda a)J_1'(\lambda b)=0$.

The above equation may give the response of the dynamic water pressure to the earthquake record.

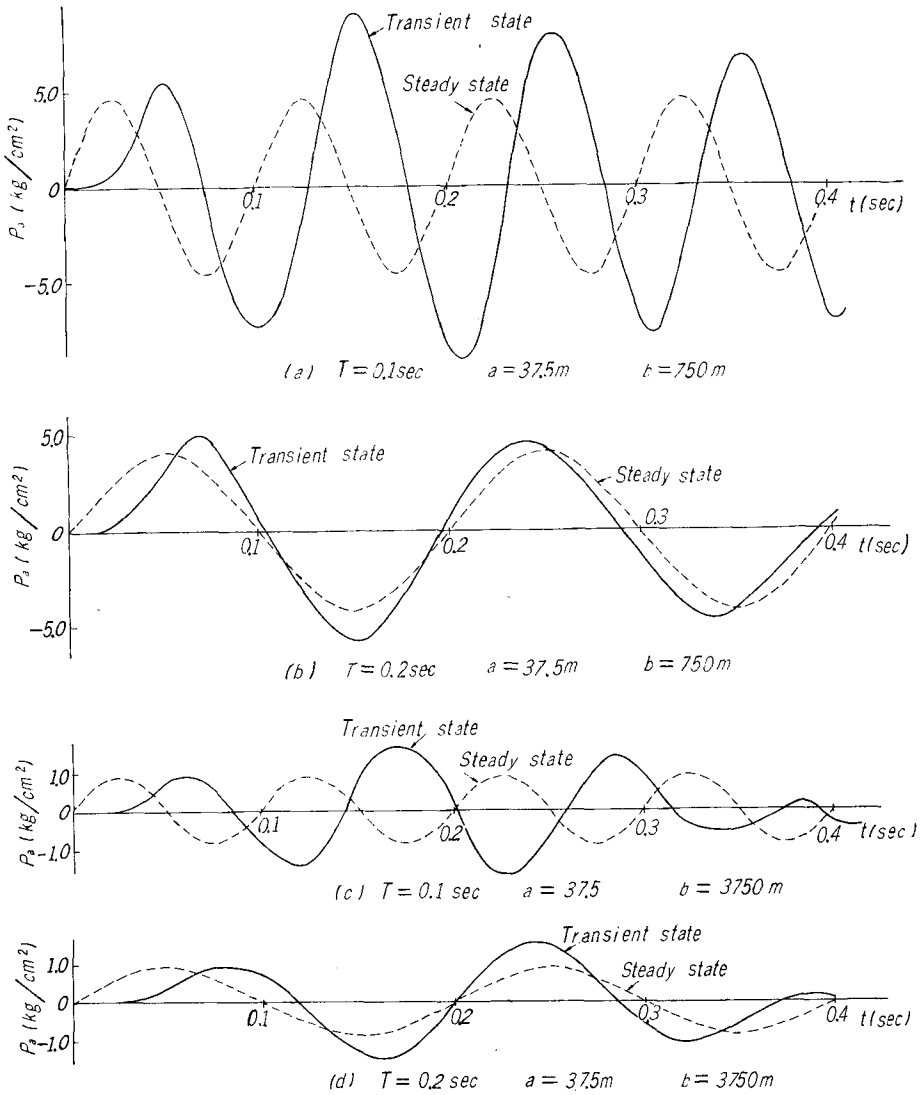

Fig. 3. Response of the dynamic water pressure,

To investigate the transient effects, the response to the excitation $f(t) = \sin \omega t$ starting from $t=0$ has been computed and is shown in Fig. 3, as an example. From these computations it may be pointed out that the maximum value of the transient dynamic water pressure is larger than that calculated by the steady state solution and that change of the dynamic water pressure does not follow proportionally to the change of acceleration with phase lag. The ratio of the maximum value of the transient dynamic water pressure to that of the steady state is illustrated in Fig. 4. As to the effect of the outside boundary, it is obvious that there are some differences of the dynamic water pressure between the case of $b=3750$ m and the case of $b=750$ m for the same excitation.

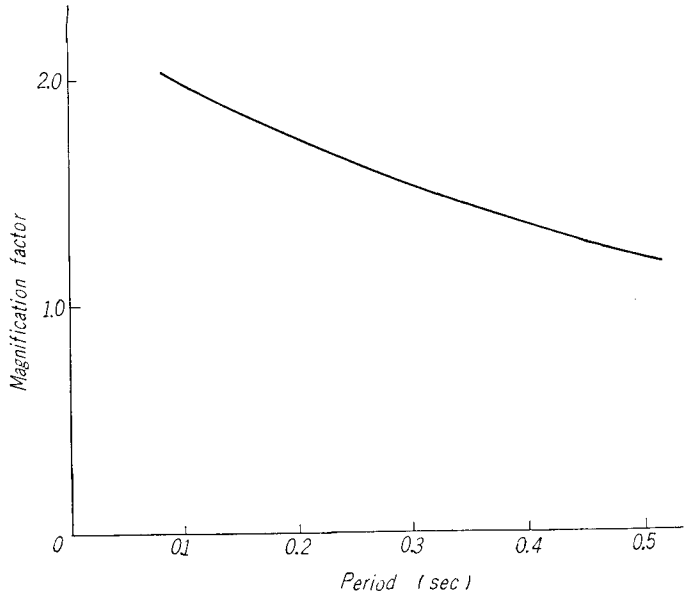

Fig. 4. Magnification factor of the transient dynamic water pressure.

3. Vibrational Characteristics of Piers in Water

3.1. Vibrational deflection of flexible piers

To investigate the vibrational characteristics of sub-merged bridge piers during earthquakes, the deflection of piers has been at first analyzed. Considering the dynamic water pressure for the force term of the differential equation governing the vibration of column, the deflection of flexible pier will be expressed by series

$$y_d = -\sum_{\xi=1}^{\infty} A_\xi \eta(k_\xi z)\, i\, e^{i\omega t}$$

where coefficient A_ξ is given by the root of the following equation.

$$(p_\eta^2/\omega^2-1)A_\eta - \sum_{\xi=1}^{\infty} A_\xi \bar{\Omega}_{\xi\eta} - i\sum_{\xi=1}^{\infty} A_\xi \tilde{\Omega}_{\xi\eta} = k_0 g\omega^2(\bar{\psi}_\eta + i\tilde{\psi}_\eta) \tag{8}$$

where

$$\bar{\Omega}_{\xi\eta} = -\sum_{m=1}^{s}\frac{\gamma_w\pi a^2}{\gamma A}\frac{4}{\lambda_m a}\frac{a_m}{A_m^2+B_m^2}\frac{1}{h}\int_0^h \eta(k_\xi z)\cos\alpha_m z dz \frac{1}{h}\int_0^h \eta(k_\eta z)\cos\alpha_m z dz$$
$$+\sum_{m=s+1}^{\infty}\frac{\gamma_w\pi a^2}{\gamma A}\frac{4}{\lambda'_m a}\frac{K_1(\lambda'_m a)}{K_0(\lambda'_m a)+K_2(\lambda'_m a)}\frac{1}{h}\int_0^h \eta(k_\xi z)\cos\alpha_m z dz \frac{1}{h}\int_0^h \eta(k_\eta z)\cos\alpha_m z dz$$

$$\bar{\psi}_\eta = \frac{1}{h}\int_0^h \eta(k_\eta z)dz - \sum_{m=1}^{s}\frac{\gamma_w\pi a^2}{\gamma A}\frac{4}{\lambda_m a}\frac{a_m}{A_m^2+B_m^2}\frac{1}{h}\int_0^h \cos\alpha_m z dz \frac{1}{h}\int_0^h \eta(k_\eta z)\cos\alpha_m z dz$$
$$+\sum_{m=s+1}^{\infty}\frac{\gamma_w\pi a^2}{\gamma A}\frac{4}{\lambda'_m a}\frac{K_1(\lambda'_m a)}{K_0(\lambda'_m a)+K_2(\lambda'_m a)}\frac{1}{h}\int_0^h \cos\alpha_m z dz \frac{1}{h}\int_0^h \eta(k_\eta z)\cos\alpha_m z dz$$

$$\tilde{\Omega}_{\xi\eta} = -\sum_{m=1}^{s}\frac{\gamma_w\pi a^2}{\gamma A}\frac{1}{\lambda_m a}\frac{b_w}{A_m^2+B_m^2}\frac{1}{h}\int_0^h \eta(k_\xi z)\cos\alpha_m z dz \frac{1}{h}\int_0^h \eta(k_\eta z)\cos\alpha_m z dz$$

$$\tilde{\psi}_\eta = -\sum_{m=1}^{s}\frac{\gamma_w\pi a^2}{\gamma A}\frac{1}{\lambda_m a}\frac{b_m}{A_m^2+B_m^2}\frac{1}{h}\int_0^h \cos\alpha_m z dz \frac{1}{h}\int_0^h \eta(k_\eta z)\cos\alpha_m z dz$$

For the convenience of investigation, when $\omega^2/c^2-\alpha_m^2<0$ which case may occur physically frequently, Eq. (8) is reduced to

$$(p_\eta^2/\omega^2-1)A_\eta = k_0 g/\omega^2\cdot\psi_\eta + \sum_{\xi=1}^{\infty}\Omega_{\xi\eta}A_\xi \tag{9}$$

where

$$\Omega_{\xi\eta} = \frac{\gamma_w\pi a^2}{\gamma A}\sum_{m=1}^{\infty}\frac{4}{\lambda'_m a}\frac{K_1(\lambda'_m a)}{K_0(\lambda'_m a)+K_2(\lambda'_m a)}\frac{1}{h}\int_0^h \eta(k_\xi z)\cos\alpha_m z dz \frac{1}{h}\int_0^h \eta(k_\eta z)\cos\alpha_m z dz$$

$$\psi_\eta = \frac{1}{h}\int_0^h \eta(k_\eta z)dz + \frac{\gamma_w\pi a^2}{\gamma A}\sum_{m=1}^{\infty}\frac{(-1)^{m-1}}{\alpha_m h}\frac{4}{\lambda'_m a}\frac{K_1(\lambda'_m a)}{K_0(\lambda'_m a)+K_2(\lambda'_m a)}\frac{1}{h}\int_0^h \eta(k_\eta z)\cos\alpha_m z dz \tag{10}$$

Although Eq. (9) is an algebraic simultaneous equation, A_ξ will be small for the higher order of ξ, except the neighbourhood of the resonance, because the term (p_η^2/ω^2-1) in the left-hand side of Eq. (9) will be large to the coefficients of A_ξ in the right-hand side. Accordingly, in an ordinary discussion except of a pier of extremely large size of dimensions, it may be sufficient to take $\xi=\eta=1$ for relatively rigid piers and $\xi=\eta=2\sim3$ for rather flexible piers.

3.2. Resonance period in water and virtual mass

The resonance period in water may be approximately given by Eq. (9) in the following form:

$$\omega_r = \frac{p_\xi}{\sqrt{1+\Omega_{\xi\xi}}} \tag{11}$$

Since p_ξ represents the natural frequency of the cantilever in air, Eq. (11) will be rewritten in the case of the transverse vibration as follows:

$$\omega_r = \sqrt{\frac{gEIk_\xi^4}{\gamma A(1+\Omega_{\xi\xi})}} \tag{12}$$

Above equation states that the resonance period in water is equivalent to the natural period of the cantilever having the virtual mass of $\gamma A\Omega_{\xi\xi}/g$. However the virtual mass takes various values under the influence of the order of the mode of the deflection.

Writing the virtual mass coefficient as $C_{v\xi}$, it will be given by the following equation:

$$C_{v\xi} = \sum_{m=1}^{\infty} \frac{4}{\lambda'_m a} \frac{K_1(\lambda'_m a)}{K_0(\lambda'_m a) + K_2(\lambda'_m a)} \left\{ \frac{1}{h} \int_0^h \eta(k_\xi z) \cos \alpha_m z dz \right\}^2 \tag{13}$$

Accordingly, the virtual mass per unit length of pier will be calculated by the product of $C_{v\xi}$ of the corresponding mode by the excluded mass of water $\gamma_w \pi a^2/g$. Although $C_{v\xi}$ depends on ω and therefore the resonance period in water have to be calculated by the try and error method, it may be the function of a/h only setting aside the compressibility of water. Value of $C_{v\xi}$ for the first mode, namely $\xi=1$, is shown in Fig. 5. On the other hand, the

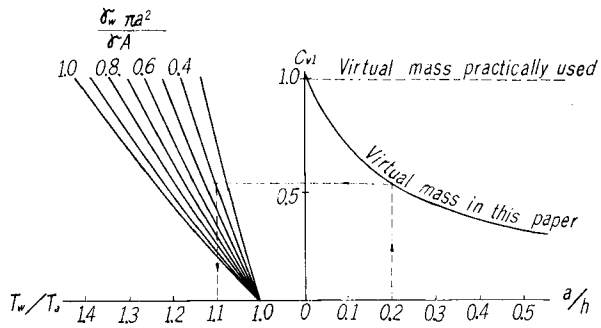

Fig. 5. Relation between the ratio of radius a to height h of piers and the resonance period T_w under water to the natural period T_a in air.

resonance period T_w in water holds the following relation with natural period T_a in air.

$$\frac{T_w}{T_a} = \sqrt{1+\Omega_{\xi\xi}} \tag{14}$$

The left side of Fig. 5 illustrates the relation of Eq. (14). Abscissa and ordinate in this figure are non-dimensional, so this figure is always applicable to cylind-

rical piers which are sub-merged to the head, fixed at the bottom and governed by the transverse vibration. Namely, the information of ratio a/h and $\gamma_w \pi a^2/\gamma A$ will give the ratio of the resonance period T_w in water to the natural period T_a in air. The dotted line, as an example, illustrates the case of the concrete pier of $a=6$ m and $h=30$ m. Moreover, the horizontal broken line represents the value of the ordinary virtual mass based on the two dimensional analysis and it indicates that the ordinary virtual mass provides excessive values.

3.3. Damping

Resistances of water acting on sub-merged bridge pier drived by earthquakes may be classified as follows:

a) Resistance induced by acceleration of piers,

b) Resistance with reference to relative velocity with water,

c) Damping force inherent to structures.

Resistance induced by acceleration may be evaluated as the dynamic water pressure and it was discussed in the preceding chapter. It is said that there are resistances varying as the square of velocity for the large Reynolds number and that varying as velocity for the small Reynolds number. The above two resistances, however, have to be considered because the Reynolds number varies successively in these vibration problems. Moreover resistance c) will not be affected by water.

The differential equation governing the transverse free vibration of sub-merged bridge piers may be written as follows:

$$EI\frac{\partial^4 y}{\partial z^4}+\frac{\gamma A}{g}\frac{\partial^2 y}{\partial t^2}+c\frac{\partial y}{\partial t}=-c^*\frac{\partial y}{\partial t}-c^{**}\,\mathrm{sgn}\,(\dot{y})\left(\frac{\partial y}{\partial t}\right)^2-P_y \tag{15}$$

Carrying out the order estimation of the work done by each resistance within small period, it may be considered that the ratio of the amplitude to the radius of the pier gives the approximate value of the ratio of the resistance proportional to the square of velocity of piers to the resistance a). Since the amplitude may be small compared with the radius, except the special case, this ratio will be so small that the resistance proportional to the square of velocity may be negligible compared with the resistance induced by acceleration. On the other hand, the following relation is established among damping constant ν, damping coefficient c^*, and natural period T.

$$\frac{\nu'}{\nu}=\frac{c^{*\prime}}{c^*}\Big/\frac{T'}{T} \tag{16}$$

where symbols with prime represent the values in water. This relation represents that ν'/ν may be apparently smaller than $c^{*\prime}/c^*$ because of $T'/T>1$

even if the damping coefficient increases from c^* to $c^{*\prime}$. Although the resistance of water is connected with the perimeter, the inertia force may be proportional to the area. Therefore, ν'/ν is inversely proportional to the radius of the pier under the condition that structural properties remain unchanged. Following the above consideration, we expect scarcely small damping effects of water regarding to the vibration of sub-merged bridge piers.

4. Model Experiment

The results of the theoretical analysis have been examined and compared with those of model experiments using three cylinders and one column made of methaacrylic acid whose specific gravity is 1.2 and Young's modulus is 2.8×10^4 kg/cm^2 (at 10°C). These models were fixed at the bottom to the horizontal plate which was forced by the shaft tied to the shaking table through the hole of the water tank of 1500 mm length, 1000 mm depth, and 1200 mm height. Then, the models are allowed to move horizontally without the rocking motion.

Table 1. Natural period in air and resonance period in water of model piers.

		(1) Natural period	(2) Resonance period in water	Ratio of (2) to (1)	Difference
Model I ϕ76 mm	Ex. value	0.050 sec	0.120 sec	2.40	0.5%
	Th. value	0.047	0.112	2.41	
Model II ϕ45 mm	Ex. value	0.090	0.155	1.85	7.5%
	Th. value	0.080	0.160	2.00	
Model III ϕ35 mm	Ex. value	0.100	0.182	1.82	5.2%
	Th. value	0.095	0.182	1.92	

(Model length : 1000 mm)

The Table 1 shows the natural periods observed by free vibration of models and those calculated by theoretical solution, and the result of the forced vibration is shown in Fig. 6. The dotted curve in Fig. 6 represents the theoretical amplitude at the top of the model I excited at the bottom by the simple harmonic motion, and

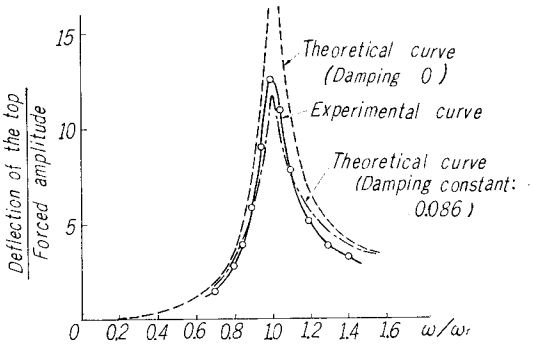

Fig. 6. Resonance curve of Model I.

damping constant 0.086 is obtained value in the free vibration. As shown in Fig. 6 the theoretical curve accords fairly with experimental one. Furthermore, the vertical strain distribution of model I is shown in Fig. 7 and that of model IV is in Fig. 8. Although the theoretical value in Fig. 8 gives excessive value, it is observed that the vertical strain distribution of dumpy column in water keeps also a good similarity to that in air.

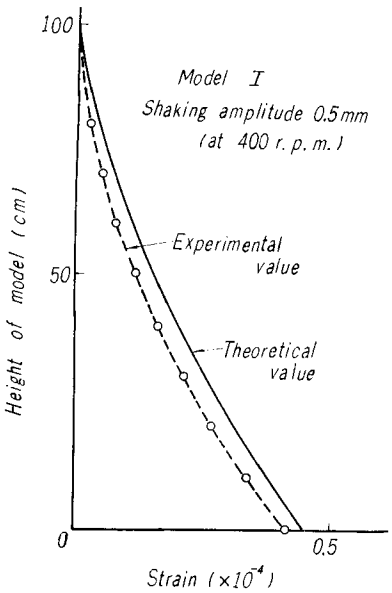

Fig. 7. The distribution of vertical strain of Model I.

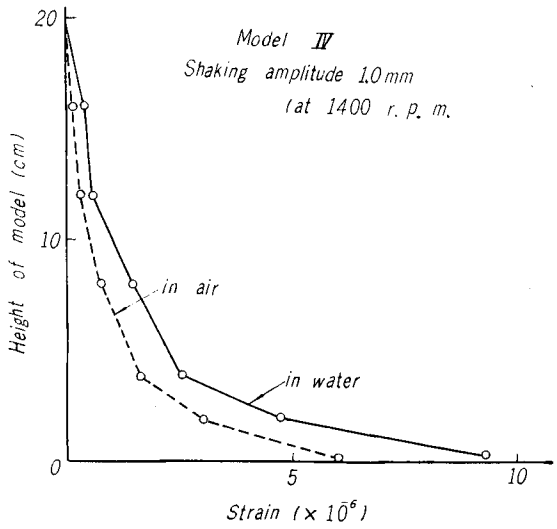

Fig. 8. The distribution of vertical strain of Model IV.

These results shown in Table 1, Fig. 6, Fig. 7, and Fig. 8 may support the appropriateness of the theoretical analysis which has been set out in this paper.

5. Aspect of Aseismic Design

Dynamic water pressures on rigid bodies will be evaluated by one of the following formulae:

a) Virtual mass

$$P_y = k_0 \gamma_w \pi a^2 \tag{17}$$

b) Westergaard

$$P_y = \frac{7}{8} k_0 \gamma_w h \sqrt{1 - z/h} \times 2a \tag{18}$$

c) Three dimensional dynamic analysis

$$P_y = k_0\gamma_w\pi a^2 \sum_{m=1}^{\infty} \frac{(-1)^{m-1}}{\alpha_m h} \frac{4}{\alpha_m a} \frac{K_1(\alpha_m a)}{K_0(\alpha_m a)+K_2(\alpha_m a)} \cos \alpha_m z \tag{19}$$

Since Eq. (17) is the result in the case of the infinitely long cylinder moving perpendicularly to its length in an infinite mass of water and Eq. (18) is on the wall structures, it should be noted that there exist some restrictions in employing these formulae for calculation. Relations among three formulae are shown in Fig. 9. In this figure, the ordinate represents the ratio of the dynamic water pressure at the bottom to the inertia force of the excluded mass of water and the abscissa is the ratio of radius of cylinder to the water depth. As seen in Fig. 9, Eq. (17), and Eq. (18) give passable approximation for small and large value of a/h, while they give excessive value for the medium value of a/h (0.5~1.0).

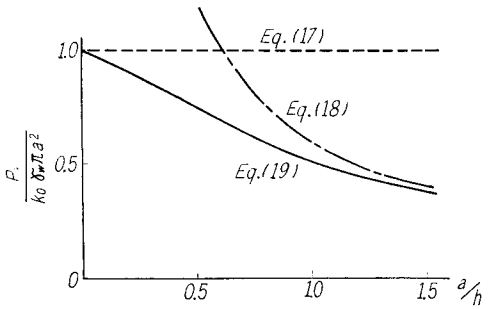

Fig. 9. Dynamic water pressure at the bottom.

The vertical distribution of the dynamic water pressure was already shown in Fig. 2. In the case of the cylinder moving in the finite mass of water, a cubic expression gives the closer approximation than a quadratic expression which was set up by Westergaard for dynamic water pressures on wall structures. Then we have following formula:

$$P_y = k_0\gamma_w\pi a^2 C \sqrt[3]{1-z/h} \tag{20}$$

Coefficient C has to be decided consulting the Fig. 9. However, since the expression $C=1-a/2h$ gives close approximation of above coefficient, Eq. (20) will be replaced by

$$P_y = k_0\gamma_w\pi a^2(1-a/2h) \sqrt[3]{1-z/h} \tag{21}$$

for the value of a/h less than 1. The above formula may be practical and useful for dynamic water pressures on cylindrical sub-merged bridge piers of finite length corresponding to exciting forces or earthquakes with long periods.

The dynamic water pressures on rigid piers may be evaluated for any arbitrary size of cylindrical piers and the specified acceleration at the foundation. We cannot, however, reduce the immediate solution of the dynamic water pressures caused by rocking or deflection of piers because rocking or deflection has to be considered in reference to dynamic properties of super-

structures and foundations. As an example, numerical computations based on the theoretical solution in this paper have been carried out and that is shown in Table 2 and Table 3. These results denote that the dynamic water pressures caused by rocking or deflection are not negligible compared with those on the rigid pier. Since this tendency is, in ordinary piers, remarkable in proportion to the ratio of the increase of the resonance period caused by the mass effect of water, the small ratio of the increase of the period is desirable from a viewpoint of the aseismic design. Moreover, the ratio of the increase of the resonance period or virtual mass should be decided in connection with not only cross sectional shape but also with water depth or the height of piers.

Table 2. Effect of rocking.

Period of ground motion (sec)			0.15	0.25	0.50
Modulus of foundation (kg/cm³)	5	y_r/y_T	1.42	1.74	391
		p_r/p_T	0.49	0.65	15.4
	10	y_r/y_T	1.56	2.53	1.44
		p_r/p_T	0.55	0.96	0.57
	20	y_r/y_T	1.96	36.8	0.47
		p_r/p_T	0.68	14.2	0.18

(Seismic coefficient : 0.25)

y_r : Displacement of the top of pier due to rocking
y_T : Displacement of the ground
p_r : Maximum value of dynamic water pressure due to rocking
p_T : Maximum value of dynamic water pressure on rigid pier

Table 3. Effect of deflection.

Period of ground motion (sec)	0.15	0.25	0.50
y_D/y_T	13.4	0.57	0.09
p_D/p_T	4.03	0.15	0.03

(Seismic coefficient : 0.25)

y_D : Deflection of the top of pier
p_T : Maximum value of dynamic water pressure due to deflection

6. Conclusions

From investigations in this paper, the following facts may be drawn out.

1) Westergaard's expression for the dynamic water pressure is not always applicable to the bridge piers. The dynamic water pressure on rigid submerged bridge pier is less than that calculated by Westergaard's formula and this tendency is remarkable in slender piers.

2) Resonance of dynamic water pressure itself does not exist on cylindrical piers isolated in water.

3) The virtual mass practically used, provides excessive value for dumpy piers and it should be decided by taking into consideration not only the cross sectional shape but also the height of piers and compressibility of water.

4) The maximum value of the transient dynamic water pressure is larger than that of the steady state. This is mainly owing to the compressibility of water and careful treatment is needed for earthquakes with short period.

5) The shore and coast should be considered in the calculation of dynamic water pressure, especially in the narrow strait or river.

6) Water resistance which is proportional to the square of relative velocity with water may be negligible compared with the resistance caused by acceleration. The damping constant in water may diminish apparently to some extent on account of the increase of the resonance period.

7) It would be safe to say that the distribution of strain or deflection curve of sub-merged bridge piers is similar to that of piers in air except the special cases.

In this paper the authors have set up a few assumptions about the mass effect of water, and the foregone formulae on the dynamic water pressure or on the virtual mass are expressed as the limiting case of the results obtained here under some special conditions. However, the damping effect caused by friction with water and the dynamic analysis taking the super-structures into consideration are not yet illustrated. Furthermore, it is needless to say that the studies on the cross-sectional shape of piers different from circle should be carried out experimentally as well as theoretically.

The contents of this paper will be presented at the Third World Conference on Earthquake Engineering, New Zealand, January 22-February 1, 1965.

References

1) Westergaard, H. M. ; "Water Pressures on Dams during Earthquakes", Trans. of A.S.C.E., Vol. 98, pp. 418-434 (1933).

2) Hatano, T. ; "Seismic Force Effect on Gravity Dam", Trans. of Japan Society of Civil Engineers, Vol. 5, pp. 83-90 (1950).

3) Kotsubo, S. ; "Dynamic Water Pressure on Dams during Earthquakes", Proc. of II W.C.E.E., Vol. 2, pp. 799-814 (1960).

4) Clough, R. W. ; "Effects of Earthquakes on Underwater Structures", Proc. of II W.C.E.E., Vol. 2, pp. 815-831 (1960).

5) Werner, P. W. and Sundquist, K. J. ; "On Hydrodynamic Earthquake Effects", Trans. of American Geophysical Union, pp. 636-657 (Oct. 1949).

6) Goto, H. and Toki, K. ; "Fundamental Studies on Vibration Characteristics and Aseismic Design of Sub-merged Bridge Piers", Proc. of Japan National Symposium on Earthquake Engineering, pp. 105-110 (Nov. 1962).

Nomenclature

ϕ : Velocity potential
t : Time
h : Water depth and height of pier
x, y : Rectangular coordinates
k_0 : Seismic coefficient
ω : Angular velocity
Y : Bessel function of the second kind
K : Modified Bessel function
τ : Time parameter in integration
c : Velocity of sound in water
$\eta(k_\xi z)$: Normal function
γ_w : Volumetic weight of water
T : Period
EI : Flexural rigidity of pier
c^* : Damping coefficient
r, θ, z : Cylindrical coordinates
a : Radius of pier
g : Acceleration of gravity
P_y : Dynamic water pressure per unit length of pier
J : Bessel function of the first kind
y_∞ : Amplitude
ρ : Specific weight of water
b : Radius of large pool
γ : Volumetic weight of pier
A : Cross sectional area of pier
ξ, η, m, l : Integers
ν : Damping constant
k_ξ : Eigen value of cantilever

Other notations are given where they appear.